A New Bio-metal-organic Framework: Synthesis, Crystal Structure and Selectively Sensing of Fe(III) Ion in Aqueous Medium①

YIN Yu-Jie FANG Wang-Jian LIU Shu-Qin②
CHEN Jun ZHANG Jian-Jun② NI Ai-Yun
(*School of Chemical Engineering, Dalian University of Technology, Dalian* 116024, *China*)

ABSTRACT A new two-dimensional (2*D*) bio-metal-organic framework based on trinuclear cluster units, $[Zn_3(adeninate)_2(CH_3COO)_4]\cdot DMF$ (**Zn–A**), was synthesized by the self-assembly of biomolecule adenines with zinc ions. Topological analysis reveals its 4^4 connected layer structure. Remarkably, **Zn–A** bears high sensitivity and selectivity detection ability of iron ion with the limit of detection being 4.0×10^{-6} mol/L.

Keywords: supramolecule, crystal structure, bio-metal-organic framework, Fe^{3+} ion, sensing;
DOI: 10.14102/j.cnki.0254-5861.2011-3180

1 INTRODUCTION

Iron, the fourth most abundant element of the earth, is widely found in nature ecosystem. Effective and rapid detection of Fe^{3+} content is of great significance for environmental protection and disease monitoring. Although traditional analytical methods, such as inductively coupled plasma mass spectrometry (ICP-MS) and chromatography, have high precision characteristics, they still suffer from the demerits of high costs and non-portability[1]. Therefore, it is particularly important and necessary to develop a faster, more convenient and low-cost approach to detect Fe^{3+}.

Luminescent metal-organic frameworks (LMOFs), a new kind of functional materials[2-5], are composed of metal ion/cluster nodes and organic ligands[6]. Their structures can be effectively regulated and optimized, enabling the effective contact with guest species to have different luminescence responses[7]. So far, many LMOFs show excellent ability in the detection of numerous guest species including Fe^{3+} ion. However, the drawback is that due to toxic aromatic ligands or metal ions, many LMOFs are bio-unfriendly, which greatly limits the practical application of LMOFs. Hence, the struggling for non-toxic LMOFs for detection applications is extensively needed to be explored and is still on the way.

Herein we selected adenine[8], a biomolecule with strong coordination ability as the ligand, and zinc ion, an element required by human body as the metal ion, and successfully isolated a new two-dimensional (2*D*) bio-MOF $[Zn_3(adeninate)_2(CH_3COO)_4]\cdot DMF$ (**Zn–A**). The luminescence sensing behaviors of **Zn–A** were investigated. The results show that it has a high sensitivity and selectivity detection ability of iron ion with the limit of detection (LOD) of 4.0×10^{-6} mol/L. Remarkably, the probe is regenerable. These results reveal the great potential of **Zn–A** in detecting of Fe^{3+}.

2 EXPERIMENTAL

2.1 Materials and methods

All the reagents and solvents were commercially purchased, and used as received without further purification. The IR spectra were recorded (400～4000 cm^{-1}) from a Nicolet-20DXB spectrometer using KBr pellets. Thermogravimetric analyses (TGA) were carried out on a TA-Q50 thermogravimetric analyzer under N_2 atmosphere with the heating rate of 10 ℃/min. Elemental analyses (C, H and N) were performed on a Vario EL III elemental analyzer, while Zn was determined on a Perkinelmer OPTIMA 2000DV inductively coupled plasma emission spectrometer. Powder X-ray diffraction patterns (PXRD) data were collected on a D/MAX-2400 X-ray diffractometer with Cu-*Kα* radiation (λ = 1.54060 Å) at a scan rate of 5 °/min. The steady state emission spectra were collected on a Hitachi F-7000 FL spectrophotometer.

2.2 Synthesis of $[Zn_3(adeninate)_2(CH_3COO)_4]\cdot DMF$ (Zn–A)

Received 16 March 2021; accepted 28 May 2021 (**CCDC 1901147**)
① This research was supported by the National Natural Science Foundation of China (21871038) and the instrumental analysis fund of DUT
② Corresponding authors. E-mail: shuqinliu@163.com and zhangjj@dlut.edu.cn

Adenine (20 mg, 0.15 mmol) and $Zn(NO_3)_2·6H_2O$ (60 mg, 0.20 mmol) were dissolved in a solvent mixture of DMF and acetic acid (5mL/1mL). Then the obtained mixture was sealed in a Teflon-lined stainless-steel vessel, and heated at 130 ℃ for 3 days under autogenous pressure. After gradually cooling to room temperature, colorless block-shaped crystals of **Zn–A** were collected by filtration, washed with DMF, and dried in air (70.28% yield based on adenine). Element analysis (%) calcd. for $C_{21}H_{27}N_{11}O_9Zn_3$: C, 32.59; H, 3.52; N, 19.91. Found: C, 32.61; H, 3.35; N, 19.92.

2. 3 Structure determination

Intensity data from single crystals of **Zn–A** were measured at 295 K on a Bruker SMART APEX II CCD area detector system with graphite-monochromated Mo-*Kα* (λ = 0.71073 Å) radiation. Data reduction and unit cell refinement were performed with Smart-CCD software. The structures were solved by direct methods using SHELXS-2014 and refined by full-matrix least-squares methods using SHELXL-2014[9]. All non-hydrogen atoms were refined anisotropically. The hydrogen atoms related to C and N atoms were generated geometrically. Crystal data: monoclinic, space group $P2_1/c$ with M_r = 773.64, a = 8.9598(4), b = 12.0398(5), c = 13.3235(6) Å, β = 94.77(3)°, V = 1433.53(11) Å^3, Z = 2, D_c = 1.792 g/cm^3, F(000) = 784, μ(Mo$K\alpha$) = 2.560 mm^{-1}, the final R = 0.0279 and wR = 0.0775 ($w = 1/[\sigma^2(F_o^2) + (0.0482P)^2 + 2.9522P]$, where $P = (F_o^2 + 2F_c^2)/3$), S = 1.117, $(\Delta/\sigma)_{max}$ = 0.001, $(\Delta\rho)_{max}$ = 0.79 and $(\Delta\rho)_{min}$ = –0.74 e/Å^3. Selected bond lengths and bond angles of **Zn–A** are given in Table 1.

Table 1. Selected Bond Lengths (Å) and Bond Angles (°) for the Compound

Bond	Dist.	Bond	Dist.	Bond	Dist.
Zn(1)–O(1)	1.976(3)	Zn(1)–N(3)	2.044(3)	Zn(2)–O(2)	2.118(3)
Zn(1)–O(3)	1.988(3)	Zn(2)–N(1)	2.114(3)	Zn(2)–O(3)	2.170(2)
Zn(1)–N(2)#1	2.025(3)	Zn(2)–N(1)#2	2.114(3)	N(2)–Zn(1)#3	2.025(3)
Angle	(°)	Angle	(°)	Angle	(°)
O(1)–Zn(1)–O(3)	104.58(11)	N(1)–Zn(2)–O(2)#2	87.70(11)	N(1)#2–Zn(2)–O(3)	90.15(10)
O(1)–Zn(1)–N(2)#1	107.02(11)	N(1)#2–Zn(2)–O(2)#2	92.30(11)	O(2)#2–Zn(2)–O(3)	91.80(10)
O(3)–Zn(1)–N(2)#1	132.19(11)	N(1)–Zn(2)–O(2)	92.30(11)	O(2)–Zn(2)–O(3)	88.20(10)
O(1)–Zn(1)–N(3)	99.75(12)	N(1)#2–Zn(2)–O(2)	87.70(11)	Zn(1)–O(3)–Zn(2)	111.25(11)

Symmetry transformations used to generate equivalent atoms: #1: x, $-y$ + 1/2, z + 1/2; #2: $-x$+2, $-y$, $-z$+1; #3: x, $-y$+1/2, z – 1/2

3 RESULTS AND DISCUSSION

3. 1 Crystal structure of Zn–A

Single-crystal X-ray diffraction analysis indicates that **Zn–A** crystallizes in the monoclinic space group $P2_1/c$ with the asymmetric unit consisting of one and a half Zn^{2+} ions, one adeninate, two coordinated acetate ions, and 1/2 lattice disordered DMF molecule. As shown in Figs. 1a, S1 and S2, Zn(1) is four-coordinated and displays a distorted tetrahedral geometry composed of two N atoms from two adeninate ligands and two O atoms from two acetate ions. Zn(2) is six-coordinated, showing a distorted octahedral configuration built by four O atoms from four acetate ions and two N atoms from two adeninate ligands. The Zn–O bonds range from 1.976(3) to 2.170(2) Å and Zn–N bond lengths fall within the range of 2.025(3)～2.114(3) Å. Each Zn(2) ion is connected to two neighbouring Zn(1) by four acetate auxiliary ligands to form the linear $Zn_3O_6N_6$ secondary building unit (SBU).

The trinuclear SBUs are connected by the adeninate linkers to form a 2*D* neutral layer that extends along the *bc* plane (Fig. 1b). In this case, the network features a 4-connected 2*D* network with 4^4 topology (Fig. 1c). Interestingly, adjacent 2*D* sheets are further connected via hydrogen bonds between the free amino groups and the uncoordinated pyrimidine nitrogen atoms with N⋯N separation and N–H⋯N angle of 2.956(4) Å and 173.6°, respectively. The existence of hydrogen bond interactions in **Zn–A** not only increases the stability of the structure, but also extends the structure into a 3*D* supramolecular framework. The solvent accessible volume of **1** without guest molecules, calculated by PLATON, is about 17.8% of the unit cell volume (255.8 Å^3 out of the 1433.5 Å^3)[10].

3. 2 Characterization of the compound

As shown in Fig. S3, the experimental pattern of **Zn–A** is highly consistent with its corresponding simulated pattern, confirming the phase purity and the crystallinity. TGA analysis reveals that it is stable below ～280 ℃ (Fig. S4). Above this temperature, it shows a striking weight loss, indicating the complete decomposition of the framework.

As shown in Fig. 2, the solid-state luminescent spectrum reveals that **Zn–A** bears a strong blue emission with maximum peaks at 438 nm. Under the same excitation

wavelength (365 nm), the adenine ligand presents an emission band centered at 416 nm. The emission of **Zn–A** can be ascribed to the adenine based emission. The red shift of **Zn–A** compared with adenine can be due to the deprotonation of adenine and the coordination interactions between adeninate and Zn^{2+} ions[11, 12]. The emission spectrum of **Zn–A** in H_2O was measured. Strong emission at 412 nm was observed. Both strong emission and excellent stability make **Zn–A** a desirable candidate for luminescent sensing.

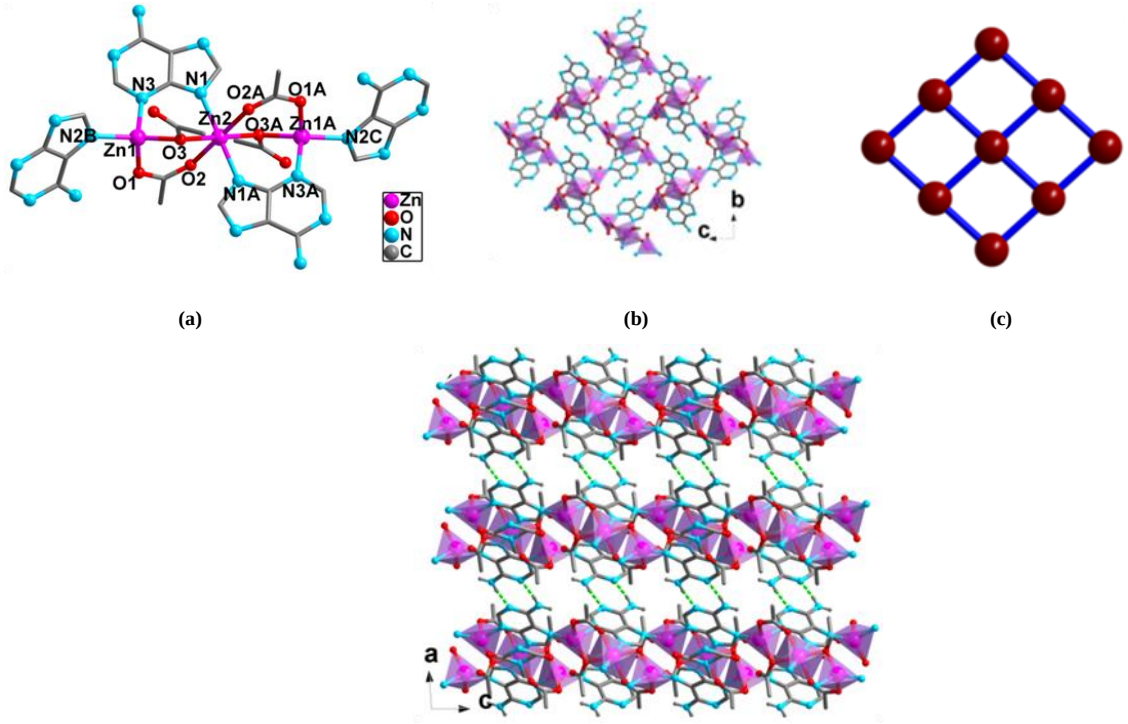

(a) **(b)** **(c)**

(d)

Fig. 1. Structure of Zn–A. (a) Coordination environment of the Zn^{II} atoms. Hydrogen atoms are omitted for clarity. Symmetry codes: A: 2 – *x*, –*y*, 1 – *z*; B: *x*, 0.5 – *y*, 0.5 + *z*; C: 2 – *x*, –0.5 + *y*, 0.5 – *z*. (b) 2*D* layer structure. (c) Representation of 4^4 topological net. (d) A view along the *b* axis of the stacking structure

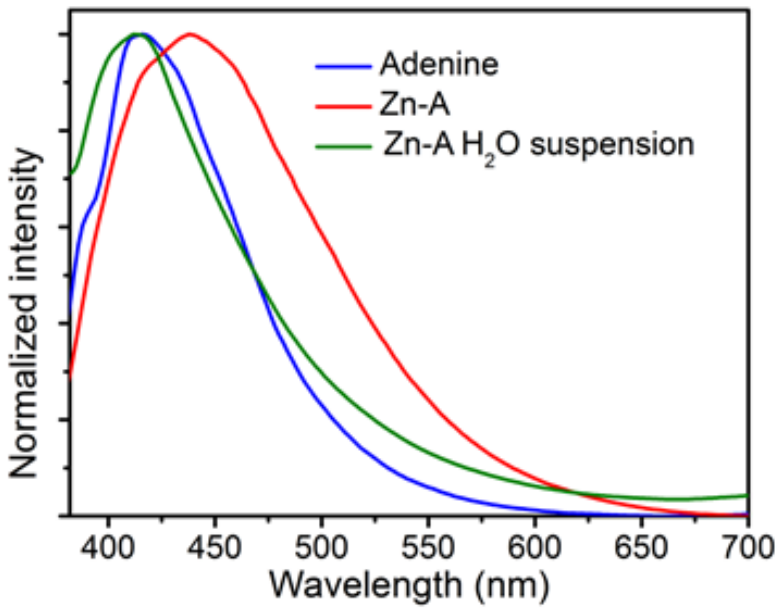

Fig. 2. Luminescence spectra of solid adenine and Zn–A and H_2O suspension of Zn–A. Excitation wavelength is 365 nm

3. 3 Luminescence sensing of Fe^{3+}

As shown in Fig. 3, the luminescence intensities of suspensions of **Zn–A** in H_2O towards different metal ions (1.0×10^{-3} mol/L) are not exactly the same. The introduction of different ions affects the luminescence intensity of **Zn–A** to a certain extent. For instance, Cd^{2+} slightly enhances the luminescence intensity, whereas the luminescence intensities are kept still in the cases of Co^{2+}, Ca^{2+} and Li^{+} (Fig. S5). However, among the rest metal ions, only Fe^{3+} bears a remarkable quenching effect, which can also be observed by naked eyes (Fig. 4) and the quenching efficiency (> 0.97) is much higher than those of other metal ions (Fig. S6).

To further examine the detection sensitivity toward Fe^{3+}, **Zn–A** was well dispersed in aqueous solutions with gradually increasing the concentration of added Fe^{3+} from 0.06 mM to 1 mM. The corresponding emission spectra were measured. As shown in Fig. 4, the luminescence intensity decreased gradually with the increase of Fe^{3+} concentration. As shown in Fig. 5, in the low concentration range ($0 \sim 3 \times 10^{-4}$ mol/L), a linear relationship was observed between the suspension's luminescence intensity and the concentration of Fe^{3+}. The corresponding correlation coefficient (R^2) is 0.987. The limit of detection (LOD) was determined as LOD = $3\sigma/K$ (where K is the slope of the linear curve and σ is the standard deviation of the luminescence intensities). The calculated LOD value was determined to be 4.0×10^{-6} mol/L.

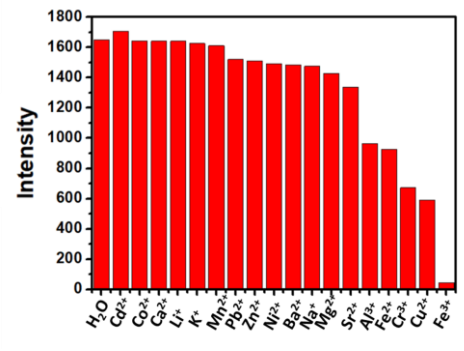

Fig. 3. Luminescence intensities of different metal cations (1.0×10^{-3} mol/L) towards the water dispersion of Zn–A

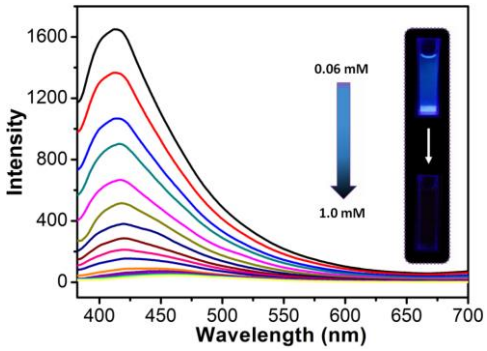

Fig. 4. Luminescence intensity of the water dispersion of Zn–A after incremental additionof Fe^{3+} solution. Excitation wavelength is 365 nm

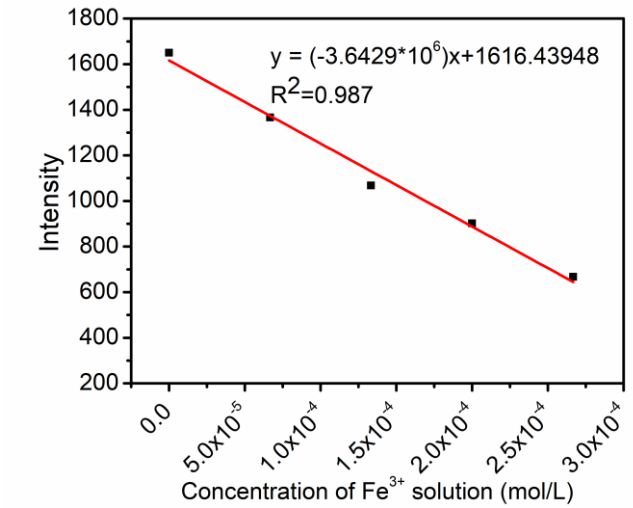

Fig. 5. Variation in the luminescence intensity of the water suspension of Zn–A as a function of the concentration of Fe^{3+} solution

The interference experiments for Fe^{3+} ion sensing were also conducted in the presence of other metal cations. The solutions of various metal cations were added individually accompanied with the addition of the solution of Fe^{3+} ion. The emission spectra of the resulting mixtures revealed that the quenching efficiency of Fe^{3+} ion did not change considerably even when other metal ions present in the sensing medium (Figs. S7 and S8). These results demonstrate that **Zn–A** bears highly anti-interference ability in sensing of Fe^{3+} ions.

It is advantageous for sensing applications if a probe can be reutilized for several times. The recycling performance

was evaluated by centrifuging Fe^{3+}@ **Zn–A** from the Fe^{3+} aqueous solution, and then washed with H_2O for several times. The results reveal that the luminescence intensity can be restored at least 3 times (Fig. S9). Remarkably, PXRD analysis shows the framework is still maintained after three cycles (Fig. S10). These results render the probe more potential in practical Fe^{3+} detection application.

The sensing mechanism was also studied. Firstly, after the cycle experiment of Fe^{3+} detection, the MOF still maintains good crystallinity, so the luminescence quenching is not caused by the collapse of the framework. To clarify the pH interference in the sensing experiments, we also test the luminescence intensities of **Zn–A** water suspensions in different pH values. The results (Fig. S11) indicate that the luminescence intensity only slightly decreases below pH = 3, confirming the quenching of **Zn–A** upon the addition of Fe^{3+} is not caused by pH but by Fe^{3+} itself. UV-Vis absorption spectrum of Fe^{3+} solution was tested (Fig. S12). The result shows the solution has a strong and wide UV-Vis adsorption band in the 300～410 nm region. Since the excitation wavelength of the above sensing experiments is 365 nm, obviously there is a competition absorption of the light source energy between the added Fe^{3+} ions and **Zn–A.** In other words, Fe^{3+} filters the light absorbed by **Zn–A** and quenches its luminescence, as also observed in the literature[13].

4 CONCLUSION

In summary, a new 2*D* bio-MOF (**Zn–A**) was synthesized by the reaction of adenine ligand and Zn^{2+} ion. The compound can be employed as probe for the selective and sensitive detection of Fe^{3+} ion in aqueous solution with LOD of 4.0×10^{-6} mol/L. This work provides a good example for the design and synthesis of CP-based probe for metal ion detection.

REFERENCES

(1) Xu, H.; Gao, J.; Qian, X.; Wang, J.; He, H.; Cui, Y.; Yang, Y.; Wang, Z.; Qian, G. Metal-organic framework nanosheets for fast-response and highly sensitive luminescent sensing of Fe^{3+}. *J. Mater. Chem. A* **2016**, 4, 10900−10905.

(2) Shi, Y.; Liu, X.; Shan, Y.; Zhang, X.; Kong, W.; Lu, Y.; Tan, Z.; Li, X. L. Naked-eye repeatable off-on-off and on-off-on switching luminescence of copper(I)-1H-imidazo[4,5-f][1,10]phenanthroline complexes with reversible acid-base responses. *Dalton Trans.* **2019**, 48, 2430−2441.

(3) Jiang, X. F.; Han, S. D.; Wang, A. N.; Pan, J.; Wang, G. M. The tri(imidazole)-derivative moiety: a new category of electron acceptors for the design of crystalline hybrid photochromic materials. *Chem. Eur. J.* **2021**, 27, 1410−1415.

(4) Feng, X.; Feng, Y. Q.; Guo, N.; Sun, Y. L.; Zhang, T.; Ma, L. F.; Wang, L. Y. Series *d-f* heteronuclear metal-organic frameworks: color tunability and luminescent probe with switchable properties. *Inorg. Chem.* **2017**, 56, 1713−1721.

(5) Ma, Y. J.; Hu, J. X.; Han, S. D.; Pan, J.; Li, J. H.; Wang, G. M. Manipulating on/off single-molecule magnet behavior in a Dy(III)-based photochromic complex. *J. Am. Chem. Soc.* **2020**, 142, 2682−2689.

(6) Ju, P.; Liu, X. C.; Zhang, E. S. A novel 3*D* Zn-based luminescence metal-organic framework: synthesis, structure and fluorescence enhanced sensing of ammonia vapor in air. *Chin. J. Struct. Chem.* **2020**, 39, 1458−1464.

(7) Feng, X.; Li, R.; Wang, L.; Ng, S. W.; Qin, G.; Ma, L. A series of homonuclear lanthanide coordination polymers based on a fluorescent conjugated ligand: syntheses, luminescence and sensor for pollutant chromate anion. *CrystEngComm*. **2015**, 17, 7878−7887.

(8) An, J.; Geib, S. J.; Rosi, N. L. Cation-triggered drug release from a porous zinc-adeninate metal-organic framework. *J. Am. Chem. Soc.* **2009**, 131, 8376−7.

(9) Sheldrick, G. M. *SHELXL-2014/7: Program for the Solution of Crystal Structures.* University of Göttingen, Göttingen **2014**.

(10) Spek, A. L. Platon squeeze: a tool for the calculation of the disordered solvent contribution to the calculated structure factors. *Acta Crystallogr., Sect. C: Struct. Chem.* **2015**, 71, 9−18.

(11) Li, B.; Fang, W. J.; Liu, S. Q.; Zhao, H.; Zhang, J. J. Two novel coordination polymers with (6, 3) topology constructed by an imidazole-containing isophthalic ligand: syntheses, structures and luminescence properties. *Chin. J. Struct. Chem.* **2020**, 39, 110−117.

(12) Li, M. Y.; Fang, W. J.; Liu, S. Q.; Ni, J.; Zhang, J. J. Two new Zn(II)/Cd(II) one-dimensional coordination polymers based on naphthalimide dicarboxylic ligand. *Chin. J. Struct. Chem.* **2019**, 38, 1807−1813.

(13) Dong, J. P.; Li, B.; Jin, Y. J.; Wang, L. Y. Efficient detection of Fe(Ⅲ) and chromate ions in water using two robust lanthanide metal-organic frameworks. *CrystEngComm.* **2021**, 23, 1677−1683.